

# Dynamic chirality in the interacting boson fermion-fermion model

---

**Brant, Slobodan; Tonev, D.; De Angelis, G.; Ventura, A.**

*Source / Izvornik:* **Physical Review C - Nuclear Physics, 2008, 78**

**Journal article, Published version**

**Rad u časopisu, Objavljena verzija rada (izdavačev PDF)**

<https://doi.org/10.1103/PhysRevC.78.034301>

*Permanent link / Trajna poveznica:* <https://urn.nsk.hr/urn:nbn:hr:217:741748>

*Rights / Prava:* [In copyright](#) / [Zaštićeno autorskim pravom.](#)

*Download date / Datum preuzimanja:* **2024-08-04**



*Repository / Repozitorij:*

[Repository of the Faculty of Science - University of Zagreb](#)



# Dynamic chirality in the interacting boson fermion-fermion model

S. Brant,<sup>1</sup> D. Tonev,<sup>2,3</sup> G. de Angelis,<sup>2</sup> and A. Ventura<sup>4</sup><sup>1</sup>*Department of Physics, Faculty of Science, University of Zagreb, 10000 Zagreb, Croatia*<sup>2</sup>*INFN, Laboratori Nazionali di Legnaro, I-35020 Legnaro, Italy*<sup>3</sup>*Institute for Nuclear Research and Nuclear Energy, BAS, 1784 Sofia, Bulgaria*<sup>4</sup>*Ente per le Nuove tecnologie, l'Energia e l'Ambiente, I-40129 Bologna and Istituto Nazionale di Fisica Nucleare, Sezione di Bologna, Italy*

(Received 24 January 2008; published 2 September 2008)

The chiral interpretation of twin bands in odd-odd nuclei was investigated in the interacting boson fermion-fermion model. The analysis of the wave functions has shown that the possibility for angular momenta of the valence proton, neutron and core to find themselves in the favorable, almost orthogonal geometry is present, but not dominant. Such behavior is found to be similar in nuclei where both the level energies and the electromagnetic decay properties display the chiral pattern, as well as in those where only the level energies of the corresponding levels in the twin bands are close together. The difference in the structure of the two types of chiral candidates nuclei can be attributed to different  $\beta$  and  $\gamma$  fluctuations, induced by the exchange boson-fermion interaction of the interacting boson fermion-fermion model. In both cases the chirality is weak and dynamic.

DOI: [10.1103/PhysRevC.78.034301](https://doi.org/10.1103/PhysRevC.78.034301)

PACS number(s): 21.10.Re, 11.30.Rd, 21.60.Fw, 23.20.Lv

## I. INTRODUCTION

In the last decade considerable experimental and theoretical effort was invested in the research of chirality in nuclei. In the pioneering works [1–3] it was proposed that the rotation of triaxial nuclei may give rise to pairs of identical  $\Delta I = 1$  bands with the same parity in odd-odd nuclei—the chiral doublet bands. This situation can occur when the proton and neutron Fermi levels are located in the lower part of the valence proton high- $j$  (particle-like) and in the upper part of the valence neutron high- $j$  (hole-like) subshells (or vice versa), and the core is triaxial. The angular momenta of the valence particles are aligned along the short and long axes of the triaxial core, while the angular momentum of the rotational core is aligned along the intermediate axis. The three angular momenta can be arranged to form two systems that differ by intrinsic static chirality, a left- and a right-handed system. When this chiral symmetry is broken in the body-fixed frame, the restoration of the symmetry in the laboratory frame results in the occurrence of degenerate doublet  $\Delta I = 1$  bands. Pairs of bands possibly due to the breaking of the chiral symmetry have been found in the  $A \sim 105$ ,  $A \sim 130$ , and  $A \sim 190$  mass regions, the most typical examples being odd-odd nuclei in the  $A \sim 130$  mass region. There the yrast and side bands are built on the  $\pi h_{11/2}$  particle-like  $\otimes \nu h_{11/2}$  hole-like configuration. In the present paper we shall analyze this case, but the conclusions can be applied equally well to the other two mass regions.

Due to the underlying symmetry, the pair of chiral twin bands should exhibit systematic properties [4–7]. The yrast and the side bands should be nearly degenerate. In the angular momentum region where chirality sets in (which for the  $A \sim 130$  mass region corresponds to  $(I \geq 12)$  the  $B(E2)$  values of the electromagnetic transitions deexciting analog states of the chiral twin bands should be almost equal. Correspondingly the  $B(M1)$  values should exhibit odd-even staggering, being for the  $\pi h_{11/2} \nu h_{11/2}^{-1}$  configuration much bigger for transitions deexciting states with odd spins than for transitions deexciting states with even spins. The odd-even staggers of  $B(M1)$

values result from the symmetry constraints imposed on the wave functions [5,6]. The  $B(M1)$  values for  $\Delta I = 1$  transitions connecting the side to the yrast band should have the odd-even staggering out of phase with respect to the  $B(M1)$  staggering for transitions deexciting states in the yrast and the side bands, i.e., for the  $\pi h_{11/2} \nu h_{11/2}^{-1}$  configuration  $B(M1)$  values for transition deexciting states with even spins have to be much bigger than for the deexciting states with odd spins. The last condition means that the  $B(M1)_{\text{In}}/B(M1)_{\text{Out}}$  staggering in the side band should be in phase with the  $B(M1)$  staggering in the yrast band.

The possible chiral interpretation of twin bands provides a rare opportunity to observe specific physical properties in deformed odd-odd nuclei. Several theoretical models have been applied in a number of articles, like the tilted axis cranking model [1], two quasiparticle + triaxial rotor model [1,8], core-particle-hole coupling model [4]. All these models have one assumption in common, they suppose a rigid triaxial core. On the contrary, all odd-odd nuclei in which twin bands have been observed have another characteristics in common, they are in regions of masses where even-even nuclei are  $\gamma$ -soft, i.e., effectively triaxial but not rigid. Their potential energy surface is rather flat in the  $\gamma$ -direction and the couplings with other core structures, not only the ground state band, are significant. It is evident that odd-odd nuclei in these mass regions could not reach the full requirements needed for the existence of chirality, but they can approach them, or at least retain some fingerprints of chirality.

To investigate the setting up of chirality in a certain nucleus, it is crucial to determine the  $B(E2)$  and  $B(M1)$  values, since this paper demonstrates that the  $B(E2)$  and  $B(M1)$  pattern is not a unique fingerprint of chirality. Unfortunately, such measurements have been done only for few nuclei of interest:  $^{134}\text{Pr}$ ,  $^{132}\text{La}$ , and  $^{128}\text{Cs}$ . In  $^{134}\text{Pr}$  [7,9] the  $B(M1)$  values in both partner bands behave similarly. In contrast, the intraband  $B(E2)$  strengths within the two bands differ. In the spin region where the almost degeneracy of the energy levels of the two

bands occurs, the  $B(E2)$  values for the yrast band are a factor 2 to 3 larger than those of the side band. The  $B(M1)$  staggerings in both bands and the  $B(M1)_{\text{In}}/B(M1)_{\text{Out}}$  staggering are not observed. The data for the side band in  $^{132}\text{La}$  [10] are not obtained for states of higher spin, and therefore these results can be treated as not conclusive, but the overall structure looks similar to the structure of  $^{134}\text{Pr}$ . In the case of  $^{128}\text{Cs}$  the electromagnetic decay properties display the expected chiral pattern [10]. In the present article, for shortness, the structure in which a pair of twin bands is close in excitation energy, but the electromagnetic decay properties do not show the chiral pattern, will be denoted as *case A*. The structure where the pair of twin bands is close in excitation energy and the electromagnetic decay properties display the chiral pattern, will be denoted as *case B*. Odd-odd nuclei in the  $A \sim 130$  mass region can be classified as case A or case B nuclei. In all these nuclei the cores are  $\gamma$ -soft, their odd-proton odd-mass neighbors have also a similar structure and their odd-neutron odd-mass neighbours have a similar structure, too. Therefore, there is *a priori* no evident reason why should they be different in structure, some of them being chiral (case B) and some being not chiral (case A). Either the structure of all these nuclei is not chiral, or there is a mechanism that dynamically induces chirality, in such a way that in case B it is far more pronounced than in case A.

## II. IBFFM CALCULATIONS

In this article the structure of twin bands will be described in the interacting boson fermion-fermion model (IBFFM) [11,12], in the version where there is no distinction between proton bosons and neutron bosons. The structure of  $^{134}\text{Pr}$  in the IBFFM framework has been described in Refs. [9,13] with the detailed analysis of wave functions in Ref. [7]. In the IBFFM besides the orientation in space, the deformation of the core is the additional degree of freedom. Valence quasiparticles are coupled to all structures of the boson core that are present in the basis, limited by the total boson number. For  $^{134}\text{Pr}$  the parameters for the core nucleus  $^{134}\text{Ce}$  were taken close to  $\gamma$ -soft values. The triaxial equilibrium deformation was generated by the cubic (three-body) term [14,15] added to the standard IBM-1 core Hamiltonian. The minimum of potential energy surface was still very shallow in the  $\gamma$ -direction and also rather broad in the  $\beta$ -direction. The fermion basis consisted of  $\pi h_{11/2}$ ,  $\pi h_{9/2}$ ,  $\pi f_{7/2}$  proton quasiparticles and  $\nu h_{11/2}$ ,  $\nu f_{7/2}$  neutron quasiparticles. The electromagnetic decay properties were found in excellent agreement with the experimental data [7,9].

A detailed analysis of the wave functions found also that the presence of configurations with the angular momenta of the proton, neutron and core in the for chirality favorable, almost orthogonal geometry, is substantial but far from being dominant. The large fluctuations of the deformation parameters  $\beta$  and  $\gamma$  around the triaxial equilibrium shape enhance the content of achiral configurations in the wave functions. The  $\beta$ -distribution of the yrast band has its maximum at larger deformations than that of the side band. At higher angular momenta, this difference becomes very pronounced.

In addition, the fluctuations of  $\beta$  in the side band become very large with increasing spin. The effective  $\gamma_{\text{eff}}$  [16], representative for an equivalent triaxially deformed rotor, in the yrast band is at smaller values than in the side band. In both bands the fluctuations of  $\gamma$  increase with spin, being more pronounced in the side band [7]. The composition of the yrast band, in terms of contributions from core states, shows that the yrast band is basically built on the ground-state band of the even-even core. With increasing spin the admixture of the  $\gamma$ -band of the core becomes more pronounced. The side band wave functions contain large components of the  $\gamma$ -band and with increasing spin, of higher-lying collective structures of the core, that near the band crossing become dominant. The conclusion of Refs. [7,9] was that the existence of twin bands in  $^{134}\text{Pr}$  should be attributed to a weak dynamic (fluctuation dominated) chirality combined with an intrinsic symmetry yet to be revealed.

In this article, as a typical representative for the  $A \sim 130$  mass, both for case A and case B, the boson core will be taken using a slightly smaller value of the cubic (three-body) term  $\Theta_3 = 0.022$  MeV in respect to the one ( $\Theta_3 = 0.030$  MeV) used for  $^{134}\text{Pr}$  [7,9]. In Refs. [7,9] the residual proton-neutron interaction was taken zero to avoid possible maskings of dominant effects in wave functions. As a consequence the signature  $S(I) = [E(I) - E(I-1)]/2I$  was opposite to the one observed in  $^{134}\text{Pr}$  and generally in this mass region. In the present work the residual proton-neutron interaction is taken as a tensor interaction  $V = V_T V(r)[3(\vec{\sigma}_\pi \cdot \vec{r}_{\pi\nu})(\vec{\sigma}_\nu \cdot \vec{r}_{\pi\nu})/r_{\pi\nu}^2 - (\vec{\sigma}_\pi \cdot \vec{\sigma}_\nu)]$  with the Gaussian radial dependence  $V(r) = \exp(-r^2/r_0^2)$  with range  $r_0 = 2.7$  fm. Since the boson-fermion interactions are derived from the quadrupole-quadrupole proton-neutron interaction, the residual proton-neutron interaction in IBFFM is an effective residual interaction, whose parameters depend on the fermion model space. In the present calculation this reflects in the range of the tensor interaction, that is larger than the bare range 1.4–2.0 fm. The role of the tensor interaction for the understanding of signature effects in deformed nuclei has been emphasized in Ref. [17]. The existence and the stability of the chiral coupling depending on the balance between particle-(deformed)core and proton-neutron particle-hole interactions, along with the triaxial shape, has already been one of the subjects of theoretical interest [18,19].

The IBFFM calculation with  $\Theta_3 = 0.022$  MeV,  $\Gamma_0^\nu = 0.75$  MeV,  $\Lambda_0^\nu = 1.6$  MeV,  $A_0^\nu = 0.1$  MeV,  $V_T = -22.0$  MeV and all other parameters as in Refs. [7,9], gives the representative structure of the case A (left panels in Fig. 1). With the residual proton-neutron interaction the staggering of the signature  $S(I)$  for yrast states with medium and high spin is in agreement with the experimental data in the  $A \sim 130$  mass region. It shows a weak staggering, being bigger for states with odd, than for those with even spins. The wave functions are not sizeably changed in respect to Refs. [7,9]. Consequently, the  $B(E2)$  and  $B(M1)$  values (left panels in Fig. 2), calculated with the same effective charges and gyromagnetic ratios as in Refs. [7,9], are very close to the values obtained in those calculations. The only difference is that the  $B(E2)$  value in the side band has now the minimum at spin 12 instead at spin 13 [7,9]. The result of the IBFFM calculation predicts

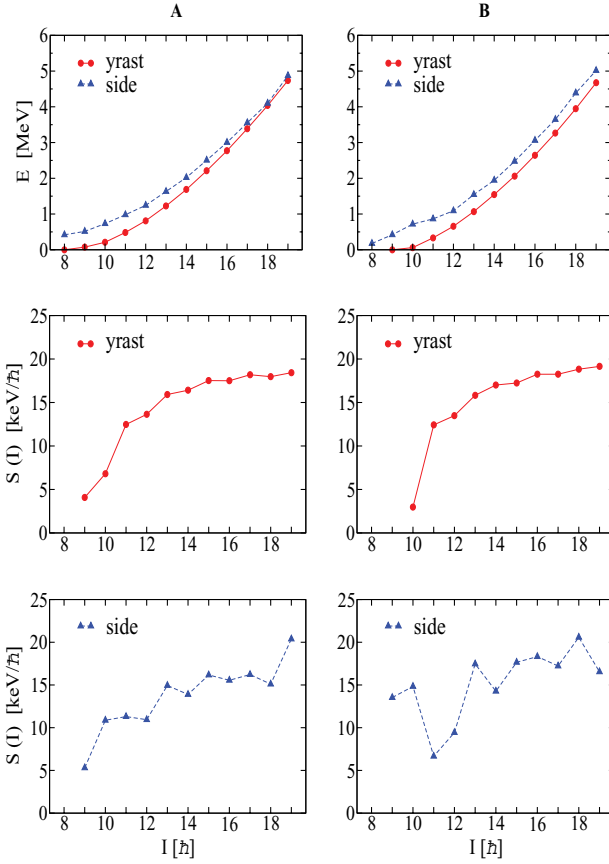


FIG. 1. (Color online) Twin bands calculated in the IBFFM for case A (left panels) and case B (right panels). In the upper panels the excitation energies of levels in the yrast and side band are presented. In the middle panels, the signature  $S(I)$  in the yrast band is displayed. In the panels on bottom the signature  $S(I)$  in the side band is presented.

the structure typical for case A: twin bands, correct signature, different  $B(E2)$  values in the two bands, absence of  $B(M1)$  staggering in both bands and a very weak  $B(M1)$  staggering for  $\Delta I = 1$  transitions from the side to the yrast band. This structure was attributed to a weak dynamic (fluctuation dominated) chirality in Ref. [7].

The same boson core allows to describe nuclei classified as case B provided one modifies the boson-fermion coupling parameters. The spin of the band head of the yrast band depends on the proton and neutron number of the nucleus through the occupation probabilities of fermion configurations. The total boson-fermion IBFFM interaction strength for each matrix element is a product of the interaction strength ( $\Gamma_0$ ,  $\Lambda_0$ , or  $A_0$  for the dynamical, exchange and monopole interaction, respectively), the fermion configuration term and the BCS term that includes fermion occupation probabilities. Therefore, the spin value of the band head of the yrast band is a result of the interplay of many factors. The structure of intermediate and high spins in the yrast and side band is, on the other hand, mainly determined by the interaction strengths. Providing  $\Gamma_0$ ,  $\Lambda_0$ , and  $A_0$  for protons and neutrons from the calculations of neighboring odd-mass nuclei, the structure of intermediate and high spin states in the yrast and side band can be investigated, and general conclusions can be obtained, without

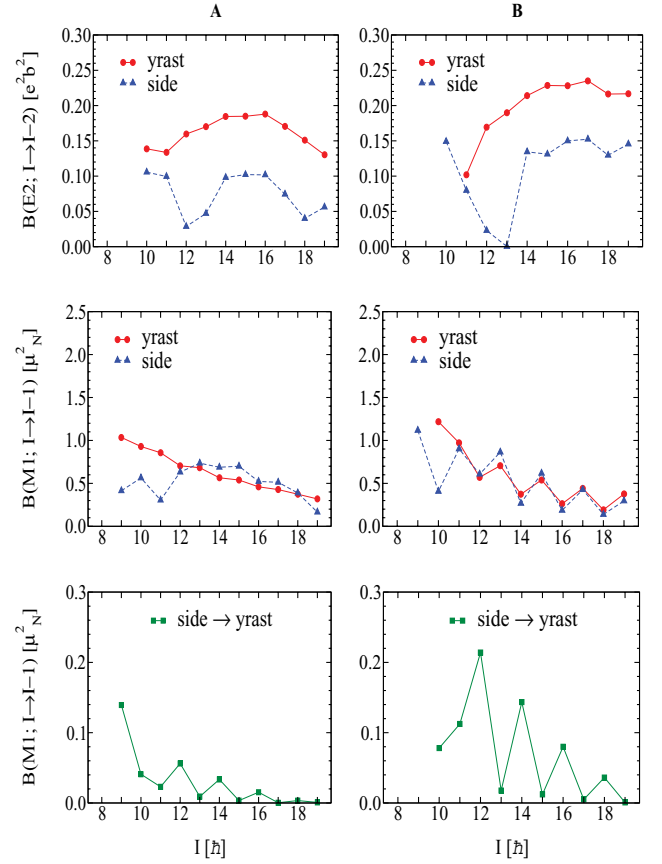


FIG. 2. (Color online)  $B(E2)$  and  $B(M1)$  values calculated in the IBFFM for case A (left panels) and case B (right panels). In the upper panels  $B(E2)$  values for transitions in the yrast and side band are presented. In the middle panels  $B(M1)$  values for transitions in the yrast and side band are shown. In the panels on the bottom  $B(M1)$  values for  $\Delta I = 1$  transitions from side to yrast band are presented.

paying attention to the spin value of the band head, as long as it is in the range of values typical for this mass region. In the present work, therefore, no fit was attempted to obtain the spin value of the band head that should be connected to a certain nucleus.

The common feature of odd-odd nuclei with twin bands is that their odd-even neighbors, with the odd fermion being a hole, have as the lowest state of the high-spin unique parity structure the  $j - 1$  state ( $[v h_{11/2}] 9/2^-$  in the  $A \sim 130$  region and  $[\pi g_{9/2}] 7/2^+$  in the  $A \sim 105$  region). In the IBFM for odd-mass nuclei this is a consequence of a strong exchange interaction. As the exchange interaction takes into account the antisymmetrization of the odd fermion with the fermion structure of the boson, it is in fact the consequence of the Pauli principle. For case B in our calculation we have taken the odd-neutron boson exchange interaction strength  $\Lambda_0^v$  still strong, but significantly weaker than in case A,  $\Lambda_0^v = 1.0$  MeV instead of 1.6 MeV for the case A. In addition, the strengths of the other two odd-neutron boson and the residual proton-neutron interaction have been reduced:  $\Gamma_0^v = 0.65$  MeV,  $A_0^v = 0.02$  MeV,  $V_T = -16.0$  MeV. All other parameters were the same as in case A. The results are presented on the right panels in Figs. 1 and 2. We refer to this calculation as case B.

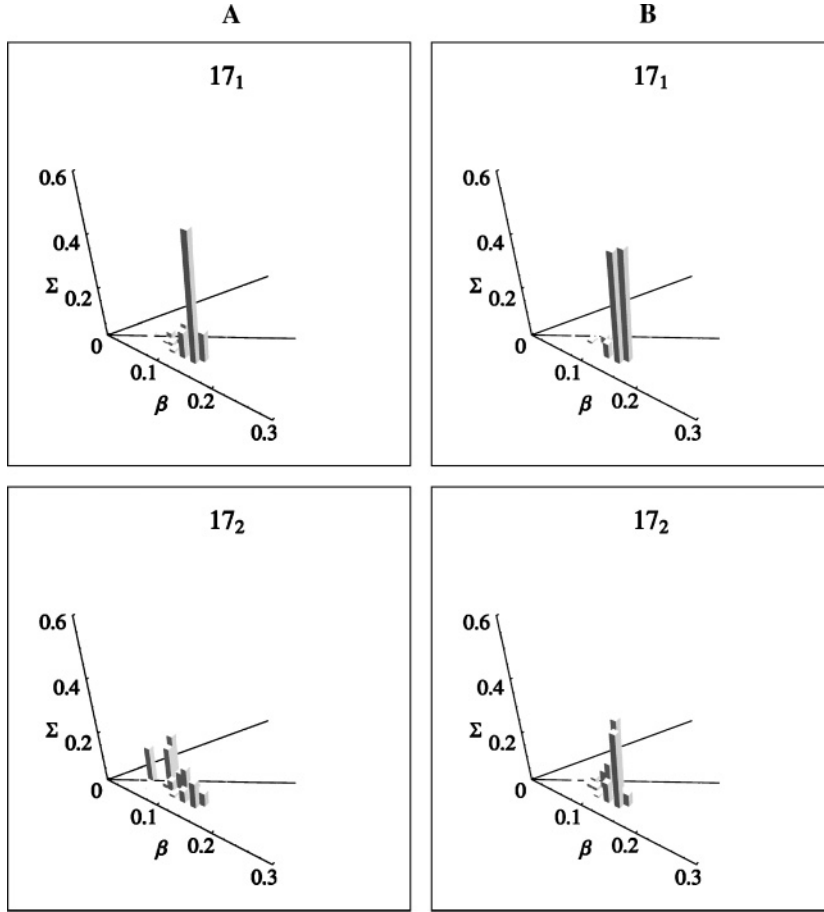


FIG. 3. IBFFM  $\beta$  and  $\gamma$  distributions, defined as in Ref. [7], for case A (left panels) and case B (right panels). In the upper panels the distributions for the yrast  $17_1$  states and in the panels on bottom for the side band  $17_2$  states are presented. The axis in the  $\beta$ - $\gamma$ -plane have  $\gamma = 0^\circ$  and  $\gamma = 60^\circ$ , while the middle line in the  $\beta$ - $\gamma$ -plane marks  $\gamma = 30^\circ$ .

In both the yrast and the side band the  $B(M1)$  values above spin  $I = 12$  exhibit the same odd-even staggering, the  $B(M1)$  values being much bigger for odd spins than for the even ones. The  $B(M1)$  values for  $\Delta I = 1$  transitions from the side to the yrast band exhibit the odd-even staggering out of phase with the  $B(M1)$  staggering in the yrast and side bands, i.e.,  $B(M1)$  values for even spins are much bigger than for the odd ones. The  $B(M1)_{\text{In}}/B(M1)_{\text{Out}}$  staggering in the side band is in phase with the  $B(M1)$  staggering in the yrast band. The effects are less pronounced than chirality requires, but are in the range of values observed in  $^{128}\text{Cs}$  [10]. The  $B(E2)$  values are not equal in the yrast and the side bands, but are closer than in case A.

### III. DISCUSSION

The distributions  $\zeta(j_\pi j_\nu)$ ,  $\psi(j_\pi R)$ , and  $\xi(j_\nu R)$  of the angles between  $\vec{j}_\pi$ ,  $\vec{j}_\nu$ , and  $\vec{R}$ , and the  $\sigma$  distribution (details of the procedure can be found in Ref. [7]), for case B show no significant differences in respect to case A [7]. In both cases the presence of configurations with the angular momenta of the proton, neutron and core in the favorable, almost orthogonal geometry, is substantial but far from being dominant. The presence of all chiral signatures in case B is not the consequence of (for chirality) more favorable geometry.

The main, but decisive, difference is revealed in the analysis of distributions in the  $\beta$ - $\gamma$ -plane. As in Ref. [7], the

deformation parameters  $\beta$  and  $\gamma$  are defined through

$$\beta^2 = \frac{\sqrt{5}(e^{\text{vib}})^2}{Z^2} \langle [Q^{\text{IBM}} \otimes Q^{\text{IBM}}]_0 \rangle, \quad (1)$$

$$\cos 3\gamma = (-) \sqrt{\frac{7}{2\sqrt{5}}} \frac{\langle (Q^{\text{IBM}} \otimes [Q^{\text{IBM}} \otimes Q^{\text{IBM}}]_2)_0 \rangle}{\langle [Q^{\text{IBM}} \otimes Q^{\text{IBM}}]_0 \rangle^{3/2}}, \quad (2)$$

where  $Q^{\text{IBM}}$  is the IBM quadrupole operator,  $Z$  the number of protons, and  $e^{\text{vib}}$  is related to the boson charge  $e_b$  through ( $e$  being the proton charge and  $R$  the radius of the nucleus):

$$e_b = \frac{3}{4\pi} e R^2 e^{\text{vib}}. \quad (3)$$

In Eqs. (1) and (2)  $\langle \text{operator} \rangle$  denotes the expectation value. The operators  $[Q^{\text{IBM}} \otimes Q^{\text{IBM}}]_0$  and  $(Q^{\text{IBM}} \otimes [Q^{\text{IBM}} \otimes Q^{\text{IBM}}]_2)_0$  are diagonalized and the IBFFM wave functions are projected onto the eigenvectors with assigned  $\beta$  and  $\gamma$ . The distributions of the projections  $\Sigma$  in the  $\beta$ - $\gamma$ -plane are presented in Fig. 3.

The  $\beta$  and  $\gamma$  distributions for cases A and B are sizably different. The two bands have significantly more similar deformations in case B than in case A (Fig. 3). The yrast bands in both cases are similar, with fluctuations on higher spins being somewhat smaller in case B. In addition, in case B components with  $\gamma$  closer to  $\gamma = 30^\circ$  are more pronounced. The side band on medium and higher spins has far less shape fluctuations and a significant decrease of components with



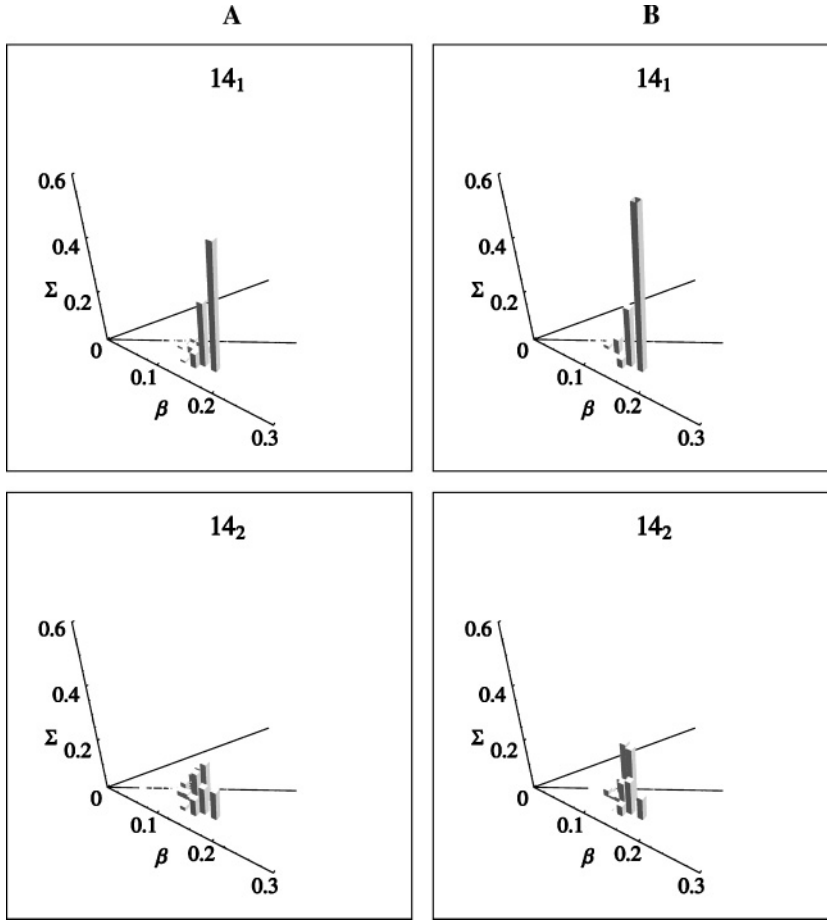


FIG. 4. IBFFM  $\beta$  and  $\gamma$  distributions, defined as in Ref. [7], for case A (left panels) and case B (right panels). In the upper panels the distributions for the yrast  $14_1$  states and in the panels on bottom for the side band  $14_2$  states are presented. The axis in the  $\beta$ - $\gamma$ -plane have  $\gamma = 0^\circ$  and  $\gamma = 60^\circ$ , while the middle line in the  $\beta$ - $\gamma$ -plane marks  $\gamma = 30^\circ$ .

small  $\beta$  in the case B. The similarities, in case B, between states of the two bands are more pronounced for odd spin members than for the even ones. In Fig. 4 the  $\beta$  and  $\gamma$  distributions are presented for the medium, even spin 14. Different deformations and larger fluctuations in the case A reflect in  $B(E2)$  values, that are much smaller in the side band than in the yrast band. In case B, due to more similar deformations, the  $B(E2)$  values for transitions between states in the side band are closer to the  $B(E2)$  values in the yrast band. Smaller shape fluctuations and more similar deformations in case B increase the probability that the two bands could be even and odd superpositions of separated left-handed and right-handed configurations, that reflects in the chiral-like behavior of  $B(M1)$  values.

The distribution of the core structure in the wave functions reveals the dynamical mechanism. In case B the weaker, but still strong, boson-fermion interactions (particularly the exchange interaction) for the neutron (hole-like) quasiparticle are not strong enough to admix big components from higher lying core bands. The ground and the  $\gamma$ -band components are dominant in the states of the side band. All chiral signatures are present, but large shape fluctuations sizably reduce their magnitude in respect to the full chiral predictions. The  $\gamma$ -softness and shape fluctuations prevent the angular momenta of the proton, neutron and core to create chiral favorable geometry on the scale they would do if the core is triaxial. For nuclei where the boson-fermion interaction is stronger, other

higher lying core structures admix into the states of the side (and partially into the yrast, too) band, increasing the shape fluctuations. This allows the admixture of more contributions from near axial shapes and consequently washes out the  $B(M1)$  staggering. The only visible signature of dynamical chirality remains the vicinity of the excitation energies of the two bands. In both cases the left-handed and right-handed sectors are not well separated. The chirality materializes only in a dynamical way, as a slow anharmonic vibration. This finding can be extended equally well to the  $A \sim 105$  and  $A \sim 190$  mass regions.

The present IBFFM calculation shows that the dominant role in the formation of different types of chiral patterns has the exchange interaction, i.e., the antisymmetrization of odd fermions with the fermion structure of the bosons. The coupling of the odd proton does not show any effect of such antisymmetrization because the occupation probability  $v^2(\pi h_{11/2}) = 0.08$  is very low. For neutrons  $v^2(vh_{11/2}) = 0.62$  is of the order where the full effect of the Pauli principle takes place. The physical foundation of chirality could therefore be beyond geometry and shape fluctuations, in the microscopic structure of twin bands.

#### IV. CONCLUSIONS

The analysis of the wave functions of chiral candidates bands in odd-odd nuclei, in the framework of the interacting

boson fermion-fermion model, shows that nuclei where both the level energies and the electromagnetic decay properties display the chiral pattern, as well as those where a pair of twin bands is only close in excitation energy, do not sizably differ in geometry. In both of them the possibility for angular momenta of the valence proton, neutron and core to find themselves in the favorable, almost orthogonal geometry is present, but not dominant. The difference in the structure of the two types of chiral candidates nuclei can be attributed to different  $\beta$  and  $\gamma$  fluctuations, induced by the exchange boson-fermion interaction of the interacting boson fermion-fermion

model. In both cases the coupling of the proton and neutron quasiparticles to the shape degrees of freedom is the dominant mechanism, leading to a weak chirality of dynamical origin.

### ACKNOWLEDGMENTS

This research has been supported by the European Commission through contract no. RII3-CT-2004-506065. D.T. is indebted to the National Science Fund at the Bulgarian Ministry of Education and Science under contract number RIC-02/2007 for a financial support.

- 
- [1] S. Frauendorf and J. Meng, Nucl. Phys. **A617**, 131 (1997).
  - [2] V. I. Dimitrov, S. Frauendorf, and F. Dönau, Phys. Rev. Lett. **84**, 5732 (2000).
  - [3] K. Starosta, T. Koike, C. J. Chiara, D. B. Fossan, and D. R. LaFosse, Nucl. Phys. **A682**, 375c (2001).
  - [4] K. Starosta, C. J. Chiara, D. B. Fossan, T. Koike, T. T. S. Kuo, D. R. LaFosse, S. G. Rohoziński, Ch. Droste, T. Morek, and J. Srebrny, Phys. Rev. C **65**, 044328 (2002).
  - [5] T. Koike, K. Starosta, C. J. Chiara, D. B. Fossan, and D. R. LaFosse, Phys. Rev. C **67**, 044319 (2003).
  - [6] T. Koike, K. Starosta, and I. Hamamoto, Phys. Rev. Lett. **93**, 172502 (2004).
  - [7] D. Tonev *et al.*, Phys. Rev. C **76**, 044313 (2007).
  - [8] I. Ragnarsson and P. Semmes, Hyperfine Interact. **43**, 423 (1988).
  - [9] D. Tonev *et al.*, Phys. Rev. Lett. **96**, 052501 (2006).
  - [10] E. Grodner *et al.*, Phys. Rev. Lett. **97**, 172501 (2006).
  - [11] S. Brant, V. Paar, and D. Vretenar, Z. Phys. A **319**, 355 (1984).
  - [12] S. Brant and V. Paar, Z. Phys. A **329**, 151 (1988).
  - [13] S. Brant, D. Vretenar, and A. Ventura, Phys. Rev. C **69**, 017304 (2004).
  - [14] K. Heyde, P. Van Isacker, M. Waroquier, and J. Moreau, Phys. Rev. C **29**, 1420 (1984).
  - [15] R. F. Casten, P. von Brentano, K. Heyde, P. Van Isacker, and J. Jolie, Nucl. Phys. **A439**, 289 (1985).
  - [16] R. V. Jolos, P. von Brentano, N. Pietralla, and I. Schneider, Nucl. Phys. **A618**, 126 (1997).
  - [17] A. Covello, A. Gargano, and N. Itaco, Phys. Rev. C **65**, 044320 (2002).
  - [18] G. Rainovski *et al.*, Phys. Rev. C **68**, 024318 (2003).
  - [19] G. Rainovski *et al.*, J. Phys. G **29**, 2763 (2003).